Sains Malaysiana 49(7)(2020): 1585-1596
http://dx.doi.org/10.17576/jsm-2020-4907-11

Kinetic, Isotherm, and Possible Mechanism of Pb(II) Ion Adsorption onto Xanthated Neem (*Azadirachta indica*) Leaf Powder

(Kinetik, Isoterma dan Mekanisme Kemungkinan Penjerapan Ion Pb(II) ke atas Serbuk Daun Mambu (*Azadirachta indica*) Terxantat)

MARDHIAH ISMAIL* & KAMAL MEGAT HANAFIAH

ABSTRACT

Adsorption capacity is one of the concern parameters in synthesizing an adsorbent for wastewater treatment. In this research, a bio-sorbent prepared by treating neem leaf powder with a chelating agent; carbon di-sulphide (CS_2) through xanthation reaction was synthesized. The effect of treating with ligand (CS_2) will be investigate since ligand will bind to metal ion. Ligand or chelating agent can help in increasing the ability of adsorbent to bind a metal ion in an aqueous solution. The chemistry of adsorption of Pb(II) ion on xanthated neem leaf powder (XNL) was investigated by using batch adsorption study. The maximum adsorption capacity, 256.41 mg g^{-1} at 318 K was determined from isotherm study, obtained from Langmuir model. FTIR spectroscopy suggested that the adsorption of Pb(II) onto XNL could possibly occur through ion exchange, Van der Wall forces and ionic interaction.

Keywords: Adsorption; isotherm; mechanisms; neem leaf; xanthate

ABSTRAK

Kapasiti penjerapan adalah salah satu parameter yang menjadi penentu dalam menghasilkan penjerap bagi merawat air buangan. Dalam kajian ini, bio-penjerap yang dihasilkan dengan merawat serbuk daun mambu dengan karbon disulfida (CS_2) melalui tindak balas xantatasi. Proses penjerapan ion Pb(II) oleh daun mambu xantat (XNL) telah dikaji menggunakan kajian penjerapan berperingkat. Kadar penjerapan maksimum ialah 256.41 mg g^{-1} diperoleh melalui kajian isoterma dengan menggunakan model Langmuir. Kajian spektroskopi FTIR mendapati penjerapan Pb(II) ke XNL berkemungkinan berlaku melalui pertukaran ion, ikatan Van der Wall dan interaksi ion.

Kata kunci: Daun mambu; isoterma; mekanisme; penjerapan; xantat

INTRODUCTION

Lead can be considered as the oldest toxin to human. Gidlow (2015) reported that these toxic cases were found since Christian era. Among latest lead toxic problem are; reproductive toxicity that will result in an increased risk of spontaneous abortion, premature delivery and low birth weight (Vigeh et al. 2010). It also can cause abnormalities in foetus development. In men, lead toxicity can reduce the concentration of sperm in semen other than caused deterioration of sperm chromatin structure (Bonde et al. 2002). Lead exposure can also cause a neurotoxicity that associated with lowered IQ point, a psychiatric problem of attention deficit hyperactivity disorder (ADHD), hearing impairment and can damage peripheral nerve function. The latest lead problem in UK occur at concentration level lower than allowable level. This need urgent review on lead pollution legislation and the release of lead-containing waste need to be as low as possible.

The uses of bio-sorbent receive special focus by researcher since it is highly potential to replace other conventional methods. Bio-sorbent is rich with biomolecules/bio-structrure that has many functional groups which can act as an active site for adsorption. Bio-sorbent provides many advantages such as low cost, readily available, high adsorption capacity and can give an added value to the biomaterial such as plant leaf (Han et al. 2009; Weng et al. 2009) and bark (Tiwari et al. 1999).

Studies have proved that chemical modification can enhance the adsorption capacity through ion-exchange and complexation. Modification that introduces sulphur-containing group such as sulphides, thiols, di-thiocarbamates, di-thiophosphates and xanthates show high affinity toward heavy metals because sulphur is a soft based that have a strong affinity for metal such as cadmium, copper, lead, nickel, and mercury. Xanthates can be synthesized by reacting an organic compound containing a hydroxyl group with carbon disulphide under caustic condition. Some of the adsorption using this modification technique include activated carbon to

removed Zn(II) was increased from 15.11 - 16.43 mg g^{-1} (Behnamfard et al. 2014), orange peel with adsorption capacity for lead of 218.34 mg g^{-1} (Liang et al. 2010) and magnetic chitosan with adsorption capacity (for Pb(II)) of 76.9 mg g^{-1} (Zhu et al. 2012) are proven had optimised adsorption capacity of metal ion from aqueous solution.

Bhattacharyya and Sharma (2004) investigated the adsorption of Pb(II) from aqueous solution using Neem leaf powder with relatively high mean value of adsorption capacity of 300.1 mg g^{-1}. The work on xanthated neem leaf powder has not yet been reported. Therefore, this study investigated the effect of adding ligand onto the neem leaf powder and to study the adsorption behaviour of Pb(II), which involved determination of adsorption rate and maximum adsorption capacity. The possible mechanism of Pb(II) adsorption on XNL would also be discussed.

Materials and Methods

Reagent

Lead nitrate of $Pb(NO_3)_2$ (M.W 331.21 g mol^{-1}) was purchased from LOBAChemie, India. A stock solution of 1000 mg L^{-1} Pb(II) was prepared by dissolving 1.6146 g of Pb $(NO_3)_2$ in 1 L volumetric flask with addition of ~7 mL nitric acid to avoid precipitation of Pb(II) ion. This stock solution was transferred into a plastic bottle for storage. The required concentration of Pb(II) solution was prepared by successive dilution. All other chemicals were of analytical reagent grade.

Adsorbent Preparation

Fresh matured neem leaves were collected from Besut, Terengganu, Malaysia. The leaves were separated from the stem and were washed with tap water several times to remove dust and impurities and finally were rinsed with deionized water. Cleaned leaves were oven dried at 60 °C overnight before being grounded and sieved to obtain a particle size of 125-300 µm. Neem leaf powder was boiled in de-ionized water for 30 min to remove dissolved material such as colour pigments and lignin and was dried in the oven overnight at 60 °C. Xanthate reaction mechanism (Figure 1) was performed using the method that has been modified from the method used by Torres-Blancas et al. (2013). A weight of 10 g boiled neem leaf powder (BNL) was stirred for 2 h in 200 mL (4 M) NaOH solution which can help to liberate new adsorption sites such as hydroxyl group facilely (Hanafiah et al. 2012; Jiang et al. 2012) through elimination of pectin, lignin, and cellulose. NaOH will dissolve the lower degree of polymerization material such as β and γ-cellulose. During xanthate treatment, the hydrogen of secondary alcohol was abstracted by hydroxide ion during treatment. A volume of 1 mL CS_2 was added into the mixture and was left to stir for another 2 h. Deprotonated of secondary alcohol will be abstracted by the electrophile of CS_2 forming a covalent bond between oxygen and carbon. The same mechanism can occur between CS_2 and carboxylate. The mixture was filtered and washed thoroughly with 500 mL deionized water 8 times. The treated adsorbent was dried in an oven at 60 °C overnight and again was grounded and sieved to obtain a particle size of 125-250 µm. This xanthated neem leaves powder was kept in an airtight container prior uses. The xanthate treated BNL was abbreviated as XNL.

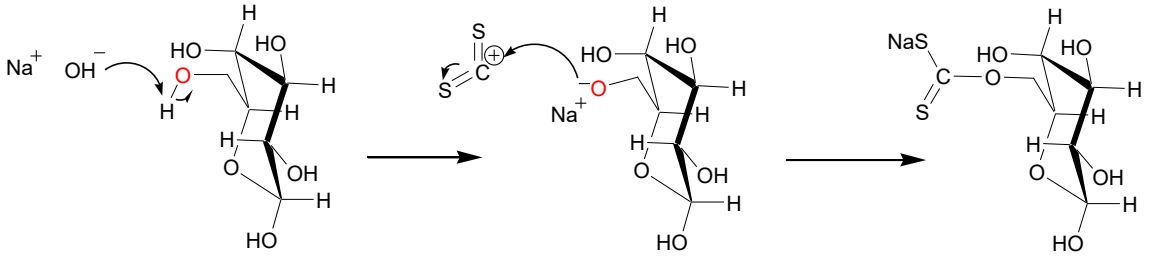

FIGURE 1. Xanthation mechanism

Adsorbent Characterization

The types of functional groups presence on the XNL surface were determined using Fourier transform infrared (FTIR) spectrometer (Spectrum 100, Perkin Elmer, USA) by scanning the sample KBr disc in the range of 450-4000 cm^{-1}. The KBr disc was prepared by mixing a fine grounded of 2 mg adsorbent with 200 mg KBr powder. The Scanning Electron Microscope (FESEM), (Supra 400, Carl Zeiss SMT, Germany) coupled with Electron Dispersive X-RAY (EDX), (Microanalysis, Oxford instrument, UK) was used to analyse the surface morphology of the XNL. The percentage by mass of the element contain in the XNL was determined using CHNS analyser (Vario Macro CHNS, Elementar-EVISA, Germany).

BATCH EXPERIMENTS

The adsorption experiments were performed to determine the optimum physiochemical parameter including pH, dosage, contact time and initial concentration using 0.02 g XNL in 50 mL of 50 mg L^{-1} Pb(II) which was stirred at temperature 298 K and agitation of 480 rpm. To study the effect of pH, the pH of the Pb(II) solution was varied between pH ranging from 2 to 5 by adding drops of 0.1 M NaOH and HNO_3. The effect of adsorbent dosage was performed by varying adsorbent dosage from 0.01 to 0.05 g while fixed the pH of Pb(II) solution at pH 4. To investigate the time required for equilibrium, the stirring time was varied between 0-120 min using three different Pb(II) concentration (50, 75 and 100 mg L^{-1}). An isotherm study was performed using initial Pb(II) concentrations from 50 to 200 mg L^{-1} at 298, 308 and 318 K. After adsorption, XNL was filtered, and the final concentration of Pb(II) was determined using Atomic Absorption Spectrometer (PinAAcle 900T, Perkin Elmer, USA). Each experiment was conducted in duplicate and the average of the duplicate was taken as the results with the RSD values for all analysis are less than 5%.

The amount of Pb(II) adsorbed (q_e, mg/g) and removed, removal (%) was calculated using equations (1) and (2), respectively:

$$q_e = \frac{C_i - C_e}{m} V \quad (1)$$

$$\text{Removal}(\%) = \frac{C_i - C_e}{C_i} x100 \quad (2)$$

where C_i and C_e are the initial and final concentrations (mg L^{-1}) of Pb(II) and m is the weight of XNL (g).

RESULTS AND DISCUSSION

XNL CHARACTERIZATION

The elemental composition of XNL is tabulated in Table 1. After performing a treatment with CS_2, the percentage of sulphur increased to 0.90% in XNL if compared to untreated BNL that is 0.18%. This increment could come from CS_2 after xanthate treatment of BNL. CS_2 are rich in sulphur contributed to the increment of percentage of sulphur in XNL. Percentage of carbon reduced 17% after treatment could be explained by the elimination of lignin by 10% of NaOH. Lignin is a carbon rich polymer (Júnior et al. 2009).

TABLE 1. The elemental compositions in XNL

Sample	Elements [%]				
	C	H	N	O	S
XNL	39.19	6.28	1.37	52.26	0.90
BNL	45.84	6.64	2.03	45.31	0.18

The SEM images for BNL, XNL, and XNL-Pb, are given in Figure 2. BNL image shows that the BNL powder has irregular shape and size. The surface of BNL is rough with irregular pattern. Xanthate treatment and Pb (II) adsorption does not change the adsorbent surface morphology. From EDX spectrum (Figure 3), there is no sulphur peak recorded in BNL spectrum, but after xanthation process a sulphur peak appears in a spectrum of XNL that could be a result of xanthate treatment. After Pb(II) adsorption, the Pb(II) peak appear in the EDX spectrum of XNL-Pb(II) loaded that prove the adsorption of Pb(II)ion onto XNL.

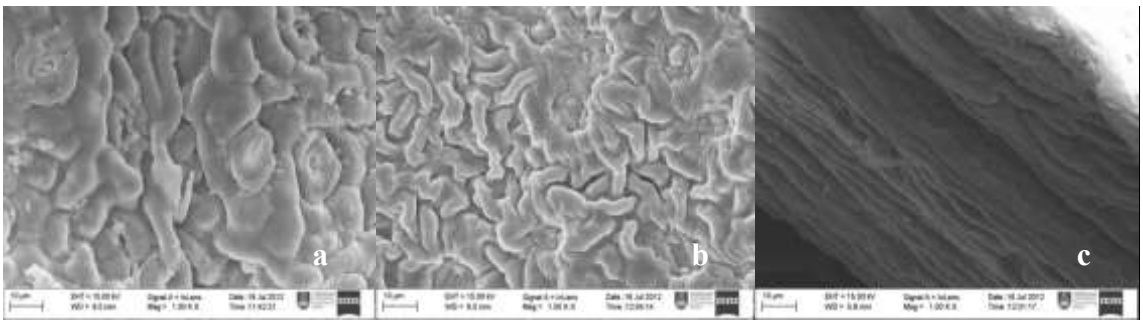

FIGURE 2. SEM images of (a) BNL, (b) XNL, and (c) XNL-Pb loaded at 1000× magnification

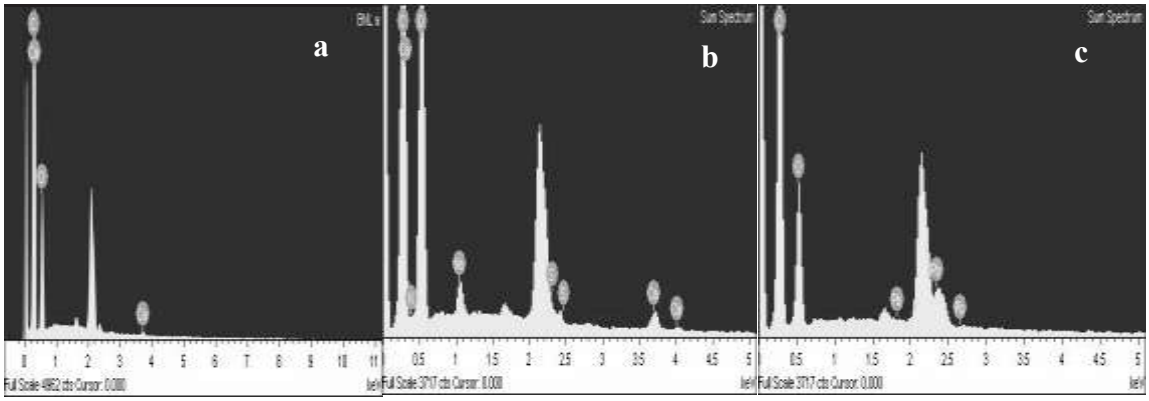

FIGURE 3. EDX spectra of (a) BNL, (b) XNL, and (c) XNL-Pb loaded

Confirmation of functional group present in the XNL and suggestion of functional groups that involved in the adsorption process were performed using FTIR spectrometer. FTIR spectra of BNL, XNL, and XNL-Pb are shown in Figure 4. BNL spectrum shows the presence of OH group at 3368 cm^{-1}. The peak at 2928 cm^{-1} can be assigned to sp^2 and sp^3 C-H stretching for most of organic material. The peak at 1723 and 1622 cm^{-1} responsible for carbonyl stretching of carboxylate and ester, respectively. The C-N bending of amine can be deduced with the peak at 1528 cm^{-1}. A C=C and C-O stretching of phenol were identified by the peaks at 1162 and 1069 cm^{-1}, respectively. After treating with CS_2, some of the peaks disappear including C=O stretching peak at 1723 cm^{-1} in BNL and a few peaks in the range of 1622 to 1069 cm^{-1} that responsible for C-O, C-N and C=C stretching due to the elimination of lignin by alkali (Teixeira et al. 2013). The presence of C-S bond in XNL can be confirmed with the absorbance at 710 cm^{-1}. Peak at 1098 cm^{-1} can be attributed to C=S stretching and peak at 1149 cm^{-1} is result from C-O-C stretching of di-thiocarbon.

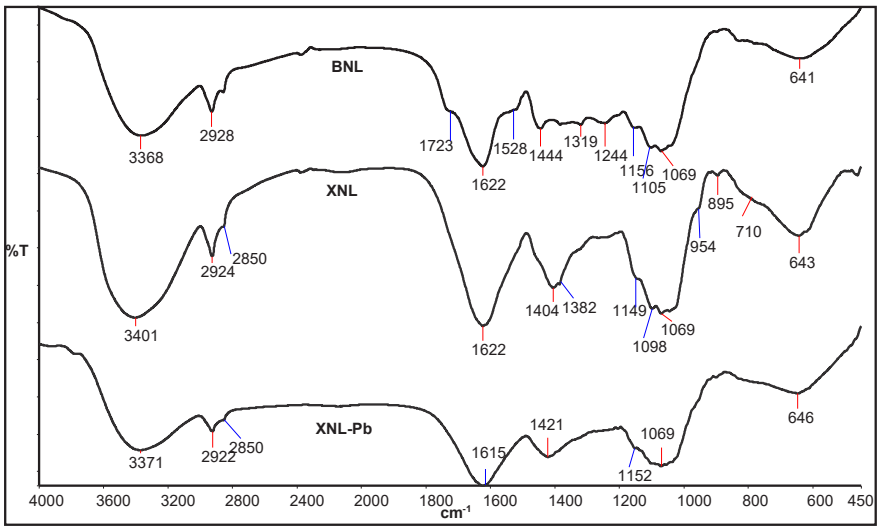

FIGURE 4. FTIR spectra of BNL, XNL, and XNL-Pb

The adsorption of Pb (II) could possibly occur (Figure 5) through electrostatic interaction attraction between negative charge of the carboxylate and positive Pb (II) ion which was deduced from the shift of carbonyl peak at 1615 to 1622 cm^{-1}. Another indication for Pb(II) adsorption is from the shift of C-O-C absorbance to a higher wavenumber. Van der Walls forces is another possible interaction of adsorption between positive Pb(II) and temporary polar induced dipole of C=O of ester.

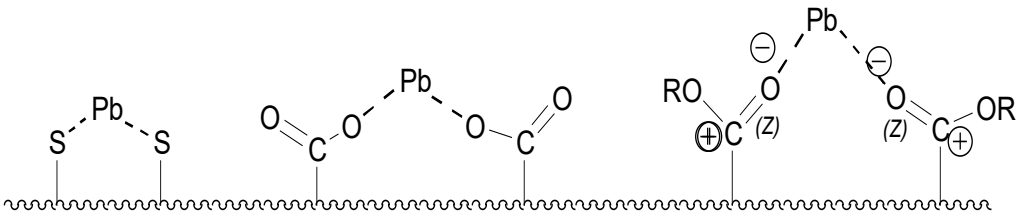

FIGURE 5. Proposed possible interaction between Pb(II) and XNL surface

EFFECT OF DOSAGE

Adsorbent dosage determines the amount of Pb(II) that can be adsorbed by XNL. The effect of adsorbent dosage was examined using five different dosages between 0.01 and 0.05 g XNL. As the amount of XNL increased, from 0.01 to 0.02 g, the percentage removal also increases from 79.96 to 98.01%. On the other hand, the adsorption capacity decreases from 199.90 to 122.51 mg g^{-1} (Figure 6). As the adsorbent increased from 0.03 to 0.05 g, percentage removal (% Removal) increased from 98.01 to 99.30%, but the adsorption capacity drop from 82.54 mg g^{-1} for 0.03 g to 49.65 mg g^{-1} for 0.05 g. High adsorption capacity at low dosage with a similar amount of adsorbate could be explained by fully occupied of all possible adsorption sites. Meanwhile, it will have low percentage removal because high number of Pb(II) ion relative to adsorbent have to compete among each other and left un-adsorbed in the bulk solution.

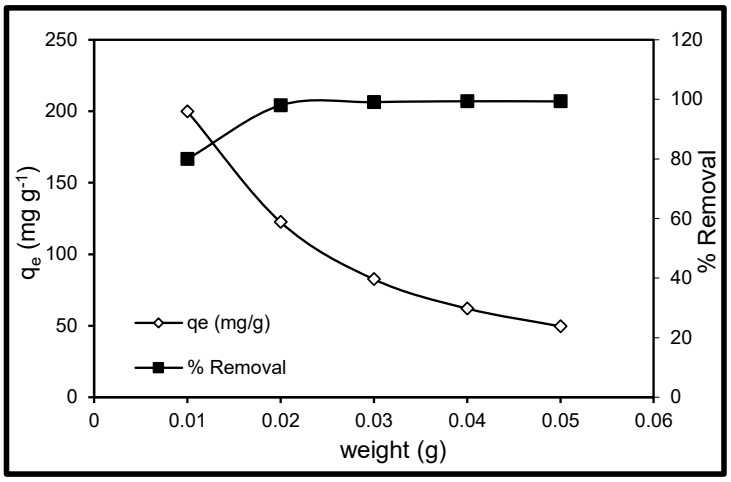

FIGURE 6. Effect of adsorbent dosage on Pb(II) adsorption onto XNL

EFFECT OF pH

The pH of the adsorbate solution also plays an important role in the adsorption process. It will affect the surface charge of the adsorbent surface which consists of a few types of functional groups such as amine, sulphate, carboxylate, and alcohol. The pH of the solution also determines the speciation of Pb ion. Pb^{2+} ion is dominant species below pH 4 while $Pb(OH)_2$ becomes dominant from pH 6 and above (Liu et al. 2011). At low pH, Pb(II) could not be adsorb because acidic pH will dissociate the adsorbed Pb (II) and return into solution. While at higher pH, Pb(II) will precipitated out from the aqueous system. As the pH increases, the adsorption capacity also increases due to the dissociation of functional groups on XNL surface that will create electrostatic attraction between negative XNL surface and positive Pb(II) ions. If the surface of the adsorbent is not fully ionized, the adsorption process will be less favoured or will be obtained with low adsorption capacity (Hanafiah et al. 2012). The pH of the solution will dictate the availability of the functional groups that can help in ion-exchange process since carboxylic group will be dissociate at higher pH (Miyoung & Mandla 2007). Consequently, it will affect the amount of Pb(II) that will be adsorbed by XNL. Since Pb (II) will start precipitate out at above pH 5, the effect of pH variation to the adsorption process was investigated from pH ranging from 2 to 5 with Pb(II) concentration of 50 mg L^{-1} (Figure 7). Maximum adsorption was obtained at pH 5. The adsorption capacity increased from 28.6 mg g^{-1} at pH 2 to 122.59 mg g^{-1} for pH 5. This phenomenon can be explained by the deprotonated of hydrogen at higher pH that make the adsorbent surface becomes negatively charge and create an electrostatic potential between negative XNL surface and positive Pb(II) ion.

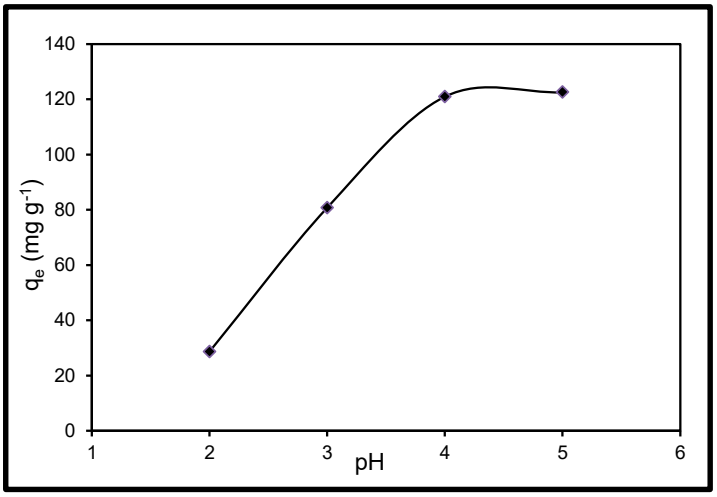

FIGURE 7. Effect of pH on Pb adsorption onto XNL

EFFECT OF INITIAL Pb CONCENTRATION AND CONTACT TIME

The amount of Pb(II) adsorbed at different initial concentration was analysed as a function of contact time to determine the equilibrium time for this system. The adsorption capacity increased with time and with increased of the initial Pb(II) concentration (Figure 8). Hanafiah et al. (2012) showed that, fast adsorption at the beginning is due to availability of many vacant adsorption sites. This adsorption sites being covered gradually with adsorbate and the adsorption rate decrease slowly and become almost constant. The equilibrium adsorption capacity increased from 120.73 mg g^{-1} for 50 mg L^{-1} to 194.26 mg g^{-1} for 100 mg L^{-1}. The increased of adsorption capacity with increasing initial Pb(II) concentration can be clarified by the increasing of effective collision between Pb(II) ion with XNL surface, this will lead to high adsorption onto XNL surface. Meanwhile, high Pb(II) concentration at the beginning stage also provide enough driving force that can overcome mass transfer resistance. The adsorption process can be divided into three stages consist of fast stage for the first 5 min, followed

by slower step between 5 and 50 min before reached equilibrium at 60 min. The first rapid step can be described as external adsorption; the second stage is intra particle diffusion and the last is the equilibrium stage with less number of effective collision because the concentration of Pb(II) ion is low (Wan Ngah et al. 2008). The equilibrium time for all three concentrations was 60 min.

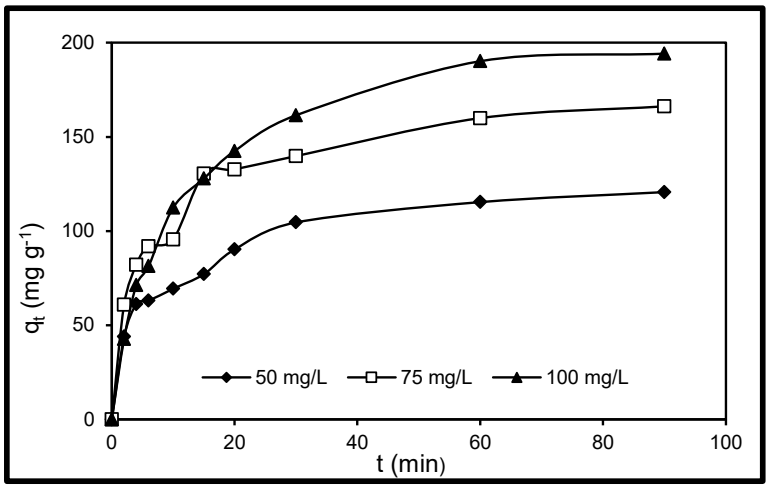

FIGURE 8. Effect of initial concentration on Pb(II) adsorption onto XNL

ADSORPTION KINETIC

Adsorption of Pb(II) onto XNL was explored by applying pseudo-first-order, pseudo-second-order and Boyd models. Pseudo-first order (Ho & McKay 1998) is given by equation below:

$$\log (q_e - q_t) = \log q_t - \frac{K_1}{2.303} t \qquad (3)$$

where q_t (mg g^{-1}) and q_e (mg g^{-1}) are the amount of Pb(II) adsorbed at time t (min) and equilibrium, respectively. K_1 (min^{-1}) is the pseudo-first order rate constant that obtained from the slope of plot of log (q_e - q_t) against t (min) (Figure 9).

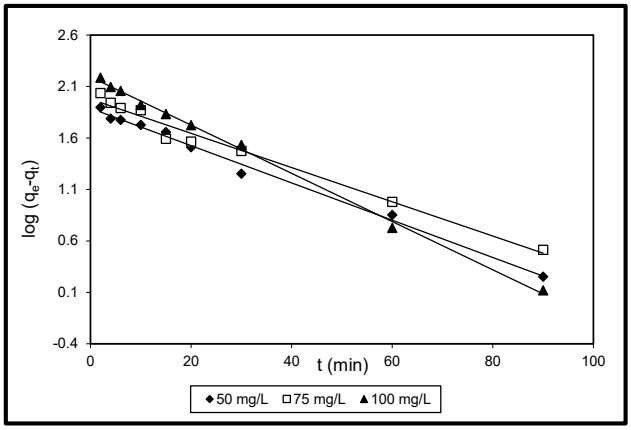

FIGURE 9. Pseudo first-order plot for adsorption of Pb onto XNL

The value of R^2 (Table 2) for all concentration of Pseudo First order plot are close to 1, but the calculated values for adsorption capacity are much different from the experimental value. Pseudo-second order (Ho & McKay 2000) is given by equation:

$$\frac{t}{q_t} = \frac{1}{h} + \frac{1}{q_e} t \qquad (4)$$

where h (mg g^{-1} min^{-1}) is the initial adsorption rate in pseudo-second order equation and can be calculated as $h=K_2qe^2$. K_2 (g $mg^{-1}min^{-1}$) is the pseudo-second-order rate constant. Pseudo-second order plot (Figure 10) are linear with R^2 close to unity and calculated adsorption capacity ($q_{e,calc}$) close to the experimental value ($q_{e,exp}$) as presented in Table 2.

The pseudo-first-order and pseudo-second-order were further quantified quantitatively using normalized standard equation, Δq (%) given by (5):

$$\Delta q\,(\%) = \sqrt{\frac{\sum\left[\left(q_{e,\exp} - q_{e,calc}\right)/q_{e,\exp}\right]^2}{n-1}}\; x\,100 \qquad (5)$$

where $q_{e,exp}$ and $q_{e,calc}$ refer to experimental and calculated adsorption capacity while n is the number of data point. According to Nasuha et al. (2010), the model with smaller Δq (%) fit well with the kinetic data. The value of normalized standard equation, Δq (%) for all concentration for both models shows that the pseudo second order has smaller values (2.51 - 6.21) than pseudo first order (14.34 - 31.11) suggested that this adsorption reaction followed closely to Pseudo-second-order model.

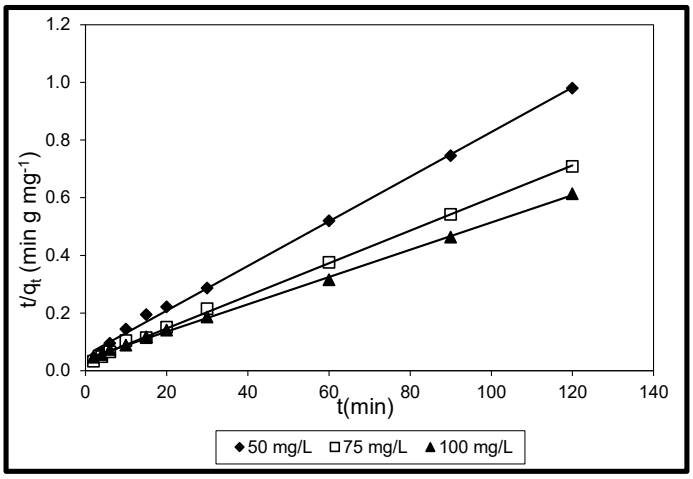

FIGURE 10. Pseudo second-order plot for adsorption of Pb onto XNL

The kinetic data was further analysed by Boyd model (Boyd et al. 1947) to deduce the actual rate determining step for this adsorption. Boyd plot was established using the following equation:

$$F = 1 - \frac{6}{\pi^2} \sum_{n-1}^{\infty} \frac{e^{n^2} B_t}{n^2} \qquad (6)$$

and

$$F = \frac{q_t}{q_\infty} \qquad (7)$$

where F is the fraction of Pb (II) adsorbed at time t and is obtained using (8), q_∞ (mg g^{-1}) is the amount of copper adsorbed at infinite time; n is an integer, and B_t is a mathematical function of F. The values of effective diffusion coefficients, D_i (cm^2 s^{-1}) can be calculated using equation (8) for F=0-0.85 and equation (9) for F>0.85.

$$B = \frac{\pi^2 D_i}{r^2} \qquad (8)$$

$$B = -0.4977 - h\left(1 - \frac{q_t}{q_\infty}\right) \qquad (9)$$

The Boyd plots (Figure 11) are not linear and do not pass the origin indicates that the film diffusion is the rate determining step which again confirmed by the value of D_i between $5.8\times10^{-6} - 7.4\times10^{-6}$ cm^2 s^{-1} (Table 1) which are much higher than the intra-particle diffusion in the range

of $10^{-11} – 10^{-13}$ cm^2 s^{-1}. This finding is again supported by the value of normalized standard equation, Δq (%) that suggests the adsorption process is best fitted to pseudo-second order model and film diffusion could be the rate determining step.

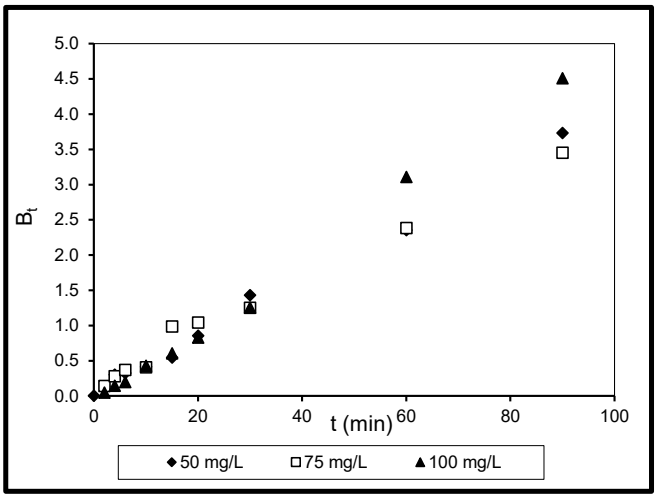

FIGURE 11. Boyd plot for adsorption of Pb onto XNL

TABLE 2. Adsorption kinetics parameters for Pb adsorption on XNL

[Pb] mg/L	Pseudo- first order					Pseudo-second order					Boyd	
	$q_{e,\,exp}$ (mg/g)	$q_{e,\,cal}$ (mg/g)	K_1 (min^{-1})	R^2	Δq (%)	h (mg/(g.min))	K_2 (min^{-1})	$q_{e,\,cal}$ (mg/g)	R^2	Δq (%)	D_i (cm^2/s)	R^2
50	122.51	77.36	0.042	0.998	26.06	18.727	0.0011	129.87	0.998	4.25	5.75×10^{-6}	0.994
75	169.42	94.89	0.038	0.981	31.11	29.499	0.0010	175.44	0.999	2.51	5.24×10^{-6}	0.988
100	195.58	155.92	0.054	0.993	14.34	24.096	0.0005	212.77	0.999	6.21	7.35×10^{-6}	0.997

EFFECT OF TEMPERATURE AND ADSORPTION ISOTHERM

Based on the general isotherm plot (Figure 12), the adsorption capacity increased with temperature from 224.63 to 254.68 mg g^{-1} which suggests that the adsorption process is endothermic. Adsorption isotherm study relates the amount of Pb(II) adsorbed by each gram of XNL (mg g^{-1}) with the concentration of Pb(II) in bulk solution (mg L^{-1}) at certain temperature at equilibrium state. This study can estimate the maximum amount of adsorbates adsorbed by a given amount of adsorbent. Once the concentration of adsorbate in adsorbent and in bulk solution is constant, the equilibrium is achieved. Adsorption mechanism and surface properties of the adsorbent can also be determined from this study.

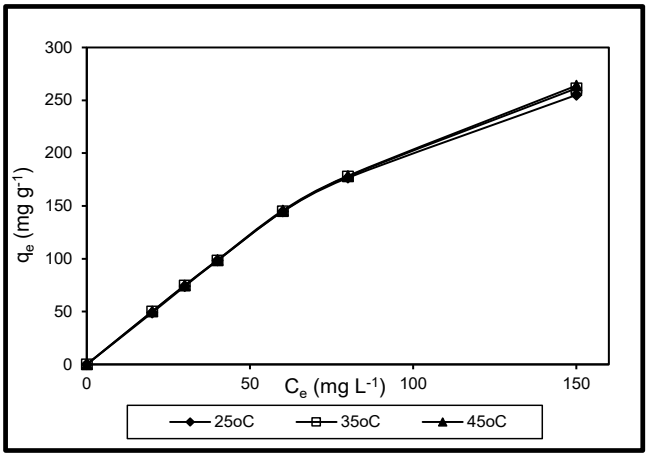

FIGURE 12. General isotherm plot for the adsorption of Pb onto XNL

Isotherm data for XNL-Pb was further analysed using Langmuir, Freundlich, and Dubinin-Reduskevich (Dubinin et al. 1947) models. Langmuir model assumes adsorption occurs at specific homogeneous sites with constant energy, and the adsorption occurs in one layer. This model is written as:

$$\frac{C_e}{q_e} = \frac{1}{q_{max} b} + \frac{C_e}{q_{max}} \qquad (10)$$

where C_e (mg/L) is the equilibrium concentration of Pb(II) in the bulk solution; q_e (mg g^{-1}) is the amount of adsorbed Pb(II); q_{max} (mg g^{-1}) is the maximum Pb(II) adsorbed; and b (L mg^{-1}) is the Langmuir constant. The slope of plot C_e/q_e versus C_e gives the maximum adsorption capacity for this system. The Langmuir plots for all temperatures (plots not shown) are linear with the maximum adsorption capacities increased with increasing temperature (Table 3) which means that the adsorption is an endothermic process.

The Freundlich isotherm model explained the adsorption process that occurs on highly heterogeneous adsorbent surface, and the adsorption can be a multi-layer adsorption on an exponential active site with different energy. This model is given by:

$$\log q_e = \log K_F + \frac{1}{n} \log C_e \qquad (11)$$

where K_F (mg/g) is the maximum adsorption capacity; and n is a parameter that relates with adsorption intensity. The plots (plots not shown) are also linear with n > 1 which means Pb(II) is favourably adsorbed onto XNL surface. The Dubinin-Reduskevich model is given by equation (12) below:

$$\ln q_e = \ln q_m - K\varepsilon^2 \qquad (12)$$

where ε (Polanyi potential) is equal to RT ln(1+1/C_e); R is the gas constant (8.314 J $mol^{-1}K^{-1}$) and T (K) is the temperature; q_m (mg g^{-1}) is the maximum adsorption capacity based on D-R isotherm; and K is related to mean adsorption energy (E in kJ mol^{-1}) given by:

$$E = \frac{1}{\sqrt{2K}} \qquad (13)$$

Dubinin-Radushkecivh (D-R) isotherm was applied to distinguish between physical and chemical adsorption.

Isotherm study suggested that the adsorption data fit Langmuir model as the values of maximum adsorption capacity q_{calc} obtained from Langmuir models were close to the experimental values (q_{exp}) (Table 3). The adsorption of Pb(II) onto XNL was a monolayer adsorption as predicted by Langmuir model with the q_{max} of Pb(II) was 256.41 at 318 K. The energy of adsorption was assumed to be uniform and no transmigration of Pb(II) ion on XNL surface.

TABLE 3. Adsorption isotherms parameter for Pb adsorption on XNL at different temperatures

Temp (K)	Langmuir					Freundlich				Dubinin-Radushkevich				
	Q_{exp} (mg/g)	Q_{max} (mg/g)	b (L/mg)	R^2	Δq (%)	K_F (mg/g)	n	R^2	Δq (%)	Q_{max} (mg/g)	K	E (kJ/mol)	R^2	Δq (%)
298	224.63	232.56	0.61	0.998	2.50	96.16	5.0	0.829	40.44	473.65	0.00164	17.46	1.000	78.39
308	244.25	243.90	0.53	0.998	0.10	135.36	7.6	0.977	31.52	478.16	0.00020	50.00	0.997	67.72
318	254.68	256.41	0.62	0.998	0.48	147.78	7.7	0.978	29.68	702.33	0.00003	129.10	0.989	124.29

Conclusion

This study shows that the introduction of sulphur atom into adsorbent does not change the adsorbent matrix as shown by SEM images. Addition of ligand (CS_2) gives relatively high adsorption capacity for removing Pb(II) ion from the aqueous system with short equilibrium time, at 60 min. Kinetic of adsorption is best explained by Pseudo second order as film diffusion. Based on spectroscopy study, the adsorption mechanism of Pb(II) with the XNL can be described through Van der Wall forces and ion exchange.

References

Behnamfard, A., Salarirad, M.M. & Vegliò, F. 2014. Removal of Zn(II) ions from aqueous solutions by ethyl xanthate impregnated activated carbons. *Hydrometallurgy* 144-145: 39-53. https://doi.org/10.1016/j.hydromet.2013.11.017.

Bhattacharyya, K.G. & Sharma, A. 2004. Adsorption of Pb(II) from aqueous solution by *Azadirachta indica* (neem) leaf powder. *Journal of Hazardous Materials* 113(1-3): 97-109. https://doi.org/10.1016/j.jhazmat.2004.05.034.

Bonde, J.P., Joffe, M., Apostoli, P., Dale, A., Kiss, P., Spano, M. & Caruso, F. 2002. Sperm count and chromatin structure in men exposed to inorganic lead: Lowest adverse effect levels. *Occupational and Environmental Medicine* 59(4): 234-242. https://doi.org/10.1136/oem.59.4.234.

Boyd, G.E., Adamson, A.W. & Myers, L.S. 1947. The exchange adsorption of ions from aqueous solutions by organic zeolites. II. Kinetics. *Journal of the American Chemical Society* 69(11): 2836-2848. https://doi.org/10.1021/ja01203a066.

Dubinin, M.M., Zaverina, E.D. & Radushkevich, L.V. 1947. Sorption and structure of active carbons. I. Adsorption of organic vapors. *Journal of Physical Chemistry* 21: 1351-1362.

Gidlow, D.A. 2015. Lead toxicity. *Occupational Medicine* 65(5): 348-356. https://doi.org/10.1093/occmed/kqv018.

Han, R., Wang, Y., Zhao, X. & Xie, F. 2009. Adsorption of methylene blue by phoenix tree leaf powder in a fixed-bed column: Experiments and prediction of breakthrough curves. *Desalination* 245(1-3): 284-297. https://doi.org/10.1016/j.desal.2008.07.013.

Hanafiah, M.A.K.M., Wan Ngah, W.S., Zolkafly, S.H., Teong, L.C. & Majid, Z.A.A. 2012. Acid blue 25 adsorption on base treated *Shorea dasyphylla* sawdust: Kinetic, isotherm, thermodynamic and spectroscopic analysis. *Journal of Environmental Sciences* 24(2): 261-268. https://doi.org/10.1016/S1001-0742(11)60764-X.

Ho, Y.S. & McKay, G. 2000. The kinetics of sorption of divalent metal ions onto sphagnum moss peat. *Water Research* 34(3): 735-742. https://doi.org/10.1016/S0043-1354(99)00232-8.

Ho, Y.S. & McKay, G. 1998. A comparison of chemisorption kinetic models applied to pollutant removal on various sorbents. *Process Safety and Environmental Protection* 76: 332-340.

Jiang, G.B., Lin, Z.T., Huang, X.Y., Zheng, Y.Q., Ren, C.C., Huang, C.K. & Huang, Z.J. 2012. Potential biosorbent based on sugarcane bagasse modified with tetraethylenepentamine for removal of eosin Y. *International Journal of Biological Macromolecules* 50(3): 707-712. https://doi.org/10.1016/j.ijbiomac.2011.12.030.

Júnior, O.K., Gurgel, L.V.A., de Freitas, R.P. & Gil, L.F. 2009. Adsorption of Cu(II), Cd(II), and Pb(II) from aqueous single metal solutions by mercerized cellulose and mercerized sugarcane bagasse chemically modified with EDTA dianhydride (EDTAD). *Carbohydrate Polymers* 77(3): 643-650. https://doi.org/10.1016/j.carbpol.2009.02.016.

Liang, S., Guo, X.Y., Feng, N.C. & Tian, Q.H. 2010. Effective removal of heavy metals from aqueous solutions by orange peel xanthate. *Transactions of Nonferrous Metals Society of China* 20: 187-191. https://doi.org/10.1016/S1003-6326(10)60037-4.

Liu, W.J., Zeng, F.X., Jiang, H. & Zhang, X.S. 2011. Adsorption of lead (Pb) from aqueous solution with *Typha angustifolia* biomass modified by $SOCl_2$ activated EDTA. *Chemical Engineering Journal* 170(1): 21-28. https://doi.org/10.1016/j.cej.2011.03.020.

Miyoung, O. & Mandla, A.T. 2007. Pelletized ponderosa pine bark for adsorption of toxic heavy metals from water. *Bioresources* 2: 66-81.

Nasuha, N., Hameed, B.H. & Mohd Din, A.T. 2010. Rejected tea as a potential low-cost adsorbent for the removal of methylene blue. *Journal of Hazardous Materials* 175(1-3): 126-132. https://doi.org/10.1016/j.jhazmat.2009.09.138.

Teixeira, R.N.P., Neto, V.O.S., Vicente, J.T., Oliveira, T.C., Melo, D.Q., Silva, M.A.A. & Nascimento, R.F. 2013. Study on the use of roasted barley powder for adsorption of Cu^{2+} ions in batch experiments and in fixed-bed columns. *Bioresources* 8: 3556-3573.

Tiwari, D., Mishra, S.P., Mishra, M. & Dubey, R.S. 1999. Biosorptive behaviour of mango (*Mangifera indica*) and neem (*Azadirachta indica*) bark for Hg^{2+}, Cr^{3+} and Cd^{2+} toxic ions from aqueous solutions: A radiotracer study. *Applied Radiation and Isotopes* 50(4): 631-642.

Torres-Blancas, T., Roa-Morales, G., Fall, C., Barrera-Díaz, C., Ureña-Nuñez, F. & Pavón Silva, T.B. 2013. Improving lead sorption through chemical modification of de-oiled allspice husk by xanthate. *Fuel* 110: 4-11. https://doi.org/10.1016/j.fuel.2012.11.013.

Vigeh, M., Yokoyama, K., Kitamura, F., Afshinrokh, M., Beygi, A. & Niroomanesh, S. 2010. Early pregnancy blood lead and spontaneous abortion. *Women Health* 50(8): 756-766. https://doi.org/10.1080/03630242.2010.532760.

Wan Ngah, W.S., Hanafiah, M.A.K.M. & Yong, S.S. 2008. Adsorption of humic acid from aqueous solutions on crosslinked chitosan-epichlorohydrin beads: Kinetics and isotherm studies. *Colloids and Surfaces B*: *Biointerfaces* 65(1): 18-24. https://doi.org/10.1016/j.colsurfb.2008.02.007.

Weng, C.H., Lin, Y.T. & Tzeng, T.W. 2009. Removal of methylene blue from aqueous solution by adsorption onto pineapple leaf powder. *Journal of Hazardous Materials* 170(1): 417-424. https://doi.org/10.1016/j.jhazmat.2009.04.080.

Zhu, Y., Hu, J. & Wang, J. 2012. Competitive adsorption of Pb(II), Cu(II) and Zn(II) onto xanthate-modified magnetic chitosan. *Journal of Hazardous Materials* 221-222: 155-161. https://doi.org/10.1016/j.jhazmat.2012.04.026.

Mardhiah Ismail*
Faculty of Applied Science
Universiti Teknologi MARA
40450 Shah Alam, Selangor Darul Ehsan
Malaysia

Mardhiah Ismail* & Kamal Megat Hanafiah
Faculty of Applied Science
Universiti Teknologi MARA
26400 Jengka, Pahang Darul Makmur
Malaysia

*Corresponding author; email: marismael@uitm.edu.my

Received: 2 August 2019
Accepted: 6 March 2020